Edinburgh Research Explorer

Soil microbial community, dissolved organic matter and nutrient cycling interactions change along an elevation gradient in subtropical China

1 **Soil microbial community, dissolved organic matter and nutrient**

2 **cycling interactions change along an elevation gradient in subtropical**

3 **China**

4

5 Shuzhen Wang[ab], Kate V. Heal[c], Qin Zhang[b], Yuanchun Yu[a], Mulualem Tigabu[d], Shide Huang[e],

6 Chuifan Zhou[ab]*

7

8 [a] *Co-Innovation Center for Sustainable Forestry in Southern China of Jiangsu Province, Key*

9 *Laboratory of Soil and Water Conservation and Ecological Restoration of Jiangsu Province,*

10 *Nanjing Forestry University, Nanjing 210037, China*

11 [b] *Forestry College, Fujian Agriculture and Forestry University, Fuzhou, 350002, Fujian Province,*

12 *China*

13 [c] *School of GeoSciences, The University of Edinburgh, Crew Building, Alexander Crum Brown*

14 *Road, Edinburgh EH9 3FF, UK*

15 [d] *Swedish University of Agricultural Sciences, Faculty of Forest Science, Southern Swedish Forest*

16 *Research Centre, P.O. Box 190, SE-234 22 Lomma, Sweden*

17 [e] *National Observation and Research Station of Fujian Wuyishan Forest*

18 *Ecosystem, Wuyishan, 354315, Fujian Province, China*

19

20

21

22

23

24 *Corresponding author contact details:

25 Nanjing Forestry University. Add: No.159 Longpan Road, Nanjing, 210037, Jiangsu, China.

26 E-mail address: zhouchuifan@163.com

27

28

ABSTRACT

To identify possible dominating processes involved in soil microbial community assembly, dissolved organic matter (DOM) and multi-nutrient cycling (MNC) interactions and contribute to understanding of climate change effects on these important cycles, we investigated the interaction of soil chemistry, DOM components and microbial communities in five vegetation zones - ranging from evergreen broad-leaved forest to alpine meadow - along an elevation gradient of 290 to 1960 m in the Wuyi Mountains, Fujian Province, China. Soil DOM composition and microbial community assembly were characterized using Fourier transform ion cyclotron resonance mass spectrometry (FT-ICR MS) and Illumina MiSeq high-throughput sequencing, respectively. Sloan's neutral model and the modified stochasticity ratio were used to infer community assembly processes. Key microbial drivers of the soil MNC index were identified from partial least squares path models. Our results showed that soil DOM composition is closely related to the vegetation types along an elevation gradient, the structure and composition of the microbial community, and soil nutrient status. Overall, values of the double bond equivalent (DBE), modified aromaticity index (AI_{mod}) increased, and H/C ratio and molecular lability boundary (MLB_L) percentage decreased with elevation. Lignins/CRAM-like structures compounds dominated soil DOM in each vegetation type and its relative abundance decreased with elevation. Aliphatic/protein and lipids components also decreased, but the relative abundance of aromatic structures and tannin increased with elevation. The alpha diversity index of soil bacteria gradually decreased with elevation, with deterministic processes dominating the microbial community assembly in the highest elevation zone. Bacterial communities were conducive to the decomposition of labile degradable DOM compounds (H/C≥1.5) at low elevation. In the cooler and wetter conditions at higher-elevation sites the relative abundance of potentially resistant soil DOM components (H/C<1.5) gradually increased. Microbial community diversity and composition were important predictors of potential soil nutrient cycling. Although higher elevation sites have higher nutrient cycling potential, soil DOM was assessed to be a more stable carbon store, with apparent lower lability and bioavailability than at lower elevation sites. Overall, this study increases understanding of the potential linkage between soil microbial community, multiple nutrient cycling and DOM fate in subtropical mountain ecosystems that can help predict the effect of climate change on soil carbon

58   sequestration and thus inform ecosystem management.

59

62

1. Introduction

64   Globally, the carbon (C) content of soil organic matter (SOM) is more than three times that of the

65   atmospheric C pool or the C storage of living terrestrial vegetation (Schmidt et al., 2011;

66   Gougoulias et al., 2014). Climate warming significantly affects the stock and stability of SOM and

67   increases the release of CO_2 from the soil carbon pool, thereby causing a positive feedback between

68   the terrestrial carbon cycle and climate change (Koven et al., 2011). Soil microorganisms play a

69   pivotal role in global C cycling (Abatenh et al., 2018), because a large proportion of SOM is derived

70   from storage and reprocessing within the microbial food web (Liang et al., 2019).

71   Although dissolved organic matter (DOM) accounts for less than 2% of SOM (Swenson et al.,

72   2015), it plays an important role in regulating nutrient cycles and soil micro-ecology as a dynamic

73   soil carbon pool (Fouché et al., 2020). Soil DOM compounds provide soluble organic substrates for

74   heterotrophic microbes and play a role in extracellular electron transfer across cell membranes,

75   changing the cellular redox state (Wang Y. H. et al., 2021). This alters the microbial niche and

76   thereby affects the composition and diversity of the functional microbial community (Li et al., 2019;

77   Mladenov et al., 2010; Wang Y. H. et al., 2021). The production and degradation of the different

78   components of DOM are inseparable from DOM-microbe interactions (Wang W. X. et al., 2021).

79   For example, low molecular mass plant-derived DOM molecules are consumed and transformed by

80   microorganisms, generating larger molecular mass DOM compounds with increasing soil depth

81   (Roth et al., 2019). Furthermore, changes in structure and composition of the microbial community

82   are tightly coupled to DOM turnover (Wu X. Q. et al., 2018). Analysis of changes in the temporal

83   and spatial distribution of DOM compounds and their chemodiversity is key for evaluating SOM

84   stabilization mechanisms. Fourier transform ion cyclotron resonance mass spectrometry (FT-ICR

85   MS) provides detailed information on various DOM compounds at the molecular level (e.g., Roth et

86   al., 2019; Wang W. X. et al., 2021; Wu X. Q. et al., 2018).

87   Artificial simulation warming experiments allow us to explore the response of SOM to

88   short-term temperature increase. For example, in a 4 °C soil warming experiment conducted for 4.5

89   years, it was reported that soil nutrient availability changed, which affected the composition and

90   metabolism processes of the microbial community (Dove et al., 2021). However, the applicability of

91   these results to understanding SOM processing under complex environmental conditions and over

92   long-time scales is questionable. Moreover, these experiments did not fully consider the impact of

93   substrate availability on microbial activities. An alternative approach is to use elevation gradients as

94   natural experiments to test the ecological and evolutionary responses of biological groups to climate

95   change (Körner, 2007). Climate, vegetation types, and soil heterogeneity vary greatly over short

96   spatial distances in mountain ecosystems (Tang et al., 2020). These differences have been exploited

97   in "temporal and spatial substitution" studies across geographic gradients (Rustad, 2008) in which

98   soil transplant experiments have been conducted along elevation gradients to explore the response

99   of surface SOM components to rising temperature (Cao et al., 2020; Luan et al., 2014).

100   Bioavailability of DOM, the most bioavailable fraction of SOM, is controlled by its intrinsic

101   characteristics, soil properties and external factors such as temperature and precipitation patterns

102   (Marschner and Kalbitz, 2003). The sharply heterogeneous environment along an elevation

103   gradient, such as precipitation, temperature, rainfall and vegetation type, may lead to variation in

104   water-extractable SOM (Huang et al., 2015). Hence, soil heterogeneity and environmental

105   variability have a great impact on the DOM inventory along elevation gradients. For example, Dai

106   et al. (2021) reported a positive correlation between the total genetic diversity of microorganisms

107   related to C cycling and elevation.

108   Niche and neutral processes are complementary in regulating the assembly of microbial

109   communities simultaneously (Chen Q. L. et al., 2021; Zhou and Ning, 2017). Niche-based theory

110   holds that the assembly of microbial community structure is controlled by deterministic processes

111   due to the different habitat preferences and fitness among microorganisms, including abiotic factors

112   (environmental filtering) and biotic interactions (such as facilitation and predation) (Chen et al.,

113   2019; Zhou and Ning, 2017). Thus, environmental heterogeneity is the dominant driver of microbial

114   assembly. Conversely, neutral theory asserts that microbial assemblage is generated by stochastic

115   processes, including probabilistic dispersal, random speciation and extinction, and ecological drift

(Zhou and Ning, 2017). A recent study showed that stochastic processes mainly determined the assembly of *phoD*-harboring bacteria (an indicator of organic phosphorus transformation) at high elevations (> 1500 m) with less environmental constraint, compared to the bacteria assembly at low elevation (< 1500 m), in the pristine Shennongjia forest, north-western Hubei Province, China (Wan et al., 2021). Nevertheless, the relationship between soil DOM compositions and its molecular properties and the assembly patterns of microbial community along subtropical elevation gradients remain largely unexplored.

Microbial community assembly determines the presence, abundance, and composition of microbes, thereby impacting multiple ecosystem functions (Wan et al., 2021; Xun et al., 2019). One of the methods for assessing ecosystem multi-functionality is to standardize and then average the values of multiple functions to a single index (Byrnes et al., 2014). The multiple nutrient cycling (MNC) index provides a quantifiable measure of an ecosystem to sustain multiple functions simultaneously (Delgado-Baquerizo et al., 2016; Jiao et al., 2018; Jiao et al., 2021). Microorganisms drive the soil nutrient cycling in terrestrial ecosystems (Zhou et al., 2023). Thus, analyzing microbial community assembly processes and DOM compounds, and investigating how microbial community diversity and composition drive soil multiple nutrient cycling, are needed for predicting the effect of climate change on soil microbial community and the drivers of soil C cycling.

The Wuyi Mountains have a distinct vertical zonation of vegetation types and strong climatic variation along an elevation gradient in subtropical south-eastern China, providing a unique experimental platform to explore soil-plant-microbial interactions (Wang et al., 2009; Wu et al., 2016). To identify the soil microbial community assembly process, diversity patterns, and soil DOM components, we applied FT ICR-MS to characterize soil DOM components, combined with Illumina MiSeq sequencing, to soil samples along an elevation gradient in the Wuyi Mountains, subtropical China. Specifically, we hypothesized that: i) the chemodiversity of DOM molecules and the content of refractory components increases with elevation due to the shift to specialized microbes with greater C degradation ability; ii) deterministic processes control soil bacterial and fungal community assembly at high elevation; iii) changes in soil microbial diversity result in variation in multi-nutrient cycling along the elevation gradient.

5

145

2. Material and methods

2.1. Site description, soil sample collection and preparation, and soil chemical analysis

Our study was conducted in the Wuyi Mountain National Nature Reserve (27°33′-27°54′ N, 117°27′-117°51′ E) in northern Fujian Province, south-eastern China. Five sites with different vegetation zones along an elevation gradient were selected, which are long-term ecological study sites described in Bu et al. (2011). The vegetation zones and elevations of the five sites were: evergreen broad-leaved forest (EB), coniferous and broad-leaved mixed forest (CB), coniferous forest (CF), subalpine dwarf forest (DF), and alpine meadow (AM), located at 290, 1070, 1400, 1800 and 1960 m above sea level, respectively. Additional information about soil type, climate (mean annual air temperature (MAT), and mean annual precipitation (MAP)) and the main plant species in each vegetation zone are in Table S1. Winter was selected as the optimal time for sampling to explore soil microbial effects on DOM as previous research in the same area reported higher soil microbial biomass in winter (He et al., 2009).

We randomly demarcated three plots (20 m × 20 m) in each vegetation zone. Eight cores (3 cm diameter) were taken in the upper 20 cm of soil in an S-shape in each plot on 19 January 2019 (in winter) at mid-slope positions. For each plot, all eight soil samples were mixed thoroughly to form a single composite sample (~1 kg) and then placed in an airtight bag. Thus 15 soil samples were generated, consisting of one composite sample from each of the three plots for each of the five vegetation zones. The samples were stored at 4 °C for transport to the laboratory within 48 hours (Roth et al., 2019). In the laboratory, fresh soil samples were sieved (2 mm) to remove gravel and plant debris.

Part of the sieved soil was air-dried at room temperature and used to determine soil pH, available phosphorus (AP) and available potassium (AK). Some of the 2-mm sieved air-dried soil was ground by hand and passed through a 0.149 mm nylon sieve and used for determination of soil total carbon (TC) and total nitrogen (TN) contents. The remaining fresh soil samples (< 2 mm) were cryopreserved at -80 °C and then thawed as required to represent "fresh" soil for determination of ammoniacal-nitrogen (NH_4^+-N), nitrate-nitrogen (NO_3^--N), dissolved organic carbon (DOC), and the characterization of DOM molecular composition and the soil microbial community. The

6

174 analysis methods for soil chemical properties and the molecular composition of soil DOM are

175 detailed in Supplementary Material Sections S1 and S2, respectively. We mixed equally the three

176 replicate soil samples at each site into one sample (Ye et al., 2020) for DOM extraction.

177

178 **2.2. Soil microbial community analysis**

179 Bacterial and fungal DNA were extracted from each fresh soil sample using a Power Soil DNA

180 Isolation Kit (MoBio Laboratories, Inc., CA). We subjected soil samples to high-throughput

181 sequencing using the Illumina Miseq PE300 sequencing platform at Beijing Allwegene Technology

182 Co., Ltd. (Beijing, China). DNA quality was detected by 1% agarose gel electrophoresis. The

183 primers 338F (5′-ACTCCTACGGGAGGCAGCAG-3′) and 806R

184 (5′-GGACTACHVGGGTWTCTAAT-3′) were used to amplify the V3–V4 region of the bacterial

185 16S rRNA. For fungal communities, the ribosomal ITS1-ITS2 region was targeted using primers

186 ITS1 (5′- CTTGGTCATTTAGAGGAAGTAA-3′) and ITS2 (5′-TGCGTTCTTCATCGATGC-3′).

187 The PCR reaction mixtures and PCR amplification procedures used for soil bacteria and fungi were

188 the same as in Zhang et al. (2022), and are detailed in Supplementary Material Section S3. Reads

189 were demultiplexed, quality-filtered, and processed to obtain valid sequences. Effective sequences

190 with a similarity of 97% were clustered into the same operational taxonomic unit (OTU).

191 Trimmomatic (v 0.36) and PEAR (v 0.9.6) were used to control the quality of raw sequence reads,

192 and the paired-end sequences were merged using Flash (v1.20) and PEAR (v0.9.6). Chimeric

193 sequences were removed with the Vsearch (v2.7.1) (uchime method) (Zhang et al., 2022). The

194 functional annotation of prokaryotic taxa (FAPROTAX) database was used for annotation of the

195 bacterial community (Sansupa et al., 2021) using the online tools

196 (http://cloud.biomicroclass.com/CloudPlatform/SoftPage/FAP).

197

198 **2.3. Soil multi-nutrient cycling analysis and DOM molecular properties**

199 We determined the soil MNC index from the seven nutrient variables measured: TC, TN, NH_4^+-N,

200 NO_3^--N, AP, AK, and DOC. The MNC value was calculated for the average value of the

201 standardized score of each soil nutrient variable, normalized for individual nutrient concentrations

202 on a common scale ranging from 0 to 1 (Jiao et al., 2021; Zhang et al., 2022) (Eqs. 1 and 2).

7

$$STD_i = \frac{X_i - X_{min}}{X_{max} - X_{min}} \qquad \text{(Eq. 1)}$$

$$MNC = \frac{\sum_{i=1}^{n} STD_i}{n} \qquad \text{(Eq. 2)}$$

where STD_i is the standardized individual soil nutrient variable i and X_i, X_{min}, and X_{max} are the individual soil nutrient concentrations and their minimum and maximum values across all soil samples, respectively. n represents the number of all nutrient variables. Classification and calculation of soil DOM molecular properties (DBE, AI_{mod}, average nominal oxidation state of carbon (NOSC), molecular lability boundary (MLB_L) percentage, and Shannon index) are detailed in Supplementary Material Section S4 and Table S2.

2.4. Data and statistical analysis

Apart from where stated, all statistical analyses were conducted using R v4.1.3 (R Core Team, 2018) and the significance level used was $P < 0.05$. Differences in soil chemical properties and the relative abundance and alpha diversity indexes of microbes were tested using one-way analysis of variance (ANOVA), with multiple comparisons among vegetation zones conducted using least significant difference (LSD) tests (SPSSv19, SPSS Inc., Chicago, IL, USA). The Shapiro-Wilk test and Levene's test were used to check that data fulfilled the normality and homogeneity of variance assumptions for ANOVA, respectively. If these assumptions were not met, we applied the non-parametric Kruskal-Wallis test with Bonferroni-adjusted P values using the "agricolae" (v1.3-5) package (de Mendiburu, 2021).

We calculated the alpha diversity indices (Chao1 index, Shannon index, and Faith's phylogenetic diversity whole tree index (Faith's PD whole tree index)) of microbial communities in each of the 15 soil samples using Qiime (v.1.8.0) (Taketani et al., 2017). Differences in microbial communities between elevations and the degree of separation between- and within- elevations were evaluated using the NMDS and analysis of similarities (ANOSIM) (Chen et al., 2019).

We calculated Spearman's rank correlation coefficients between the soil bacterial and the fungal OTUs with the top 300 relative abundances using the "Hmisc" and "igraph" packages in R. We used the False Discovery Rate (FDR) method to adjust the P values. Only correlations with absolute correlation coefficient values > 0.8 correlations and adjusted P values < 0.01 were

considered. The "igraph" package was also used to calculate the topological characteristics of the co-occurring network compared with 10,000 random networks generated according to the Erdös–Réyni model whose edges were assigned to any node with the same probability (Jiao et al., 2016). The degree distributions of the co-occurring networks were plotted to assess their form (Fig. S1). Gephi (0.9.3) (https://gephi.org/) was used to visualize the co-occurrence networks.

To assess the contribution of neutral processes to microbial community assembly, we fitted Sloan's neutral community model (NCM) to estimate the relationship between the occurrence frequency and mean relative abundance variations of OTUs, as described in detail in Jiao et al. (2021). The modified stochasticity ratio (MST) to infer microbial community assembly processes (Qiu et al., 2020) and Levins' niche breadth index were calculated for the soil microbial community using the "NST" package and the "niche.width" function in the "spaa" package (Chen Q. L. et al., 2021), respectively. The "EcolUtils" package was used to randomly arrange the occurrences of OTUs 1000 times to simulate the OTU occurrence frequency. OTUs with observed occurrence exceeding the upper 95% confidence interval were considered generalists, with those below the lower 95% confidence interval considered specialists, and the remainder considered neutral taxa (Zhang et al., 2018).

Associations between soil DOM composition and microbial OTUs were assessed by Pearson product-moment correlation analysis and visualized as co-occurrence network diagrams using Cytoscape 3.5.1. The "random-forest" package was used to identify the main microbial predictors of soil MNC values along the elevation gradient. The most important predictors were assessed as those with higher percentage increases in the MSE (mean squared error) of the variable. The "A3" package was used to assess the significance of the model with 5000 permutations of the response variables (Gao et al., 2021; Jiao et al., 2018), whilst the "rfPermute" package was used to estimate the significance of each predictor on the MNC index with 5000 trees. We used partial least squares path models (PLS-PM) through the "plspm" package to investigate the direct and indirect effects of microbial community characteristics on the MNC index. From initial modeling, variables with loading values < 0.7 and variance inflation factor (VIF) > 10 were removed, with the final PLS-PM constructed using the remaining variables (Yun et al., 2022). DOM data used in this manuscript can be found at   https://www.zenodo.org/record/8188815.

3. Results

3.1. Soil chemical properties and DOM composition along the elevation gradient

Soils were acidic and pH values were very similar among sites, ranging from mean pH of 4.55 in the subalpine dwarf forest (DF) vegetation zone to 4.73 in the alpine meadow (AM) zone (Table 1). Soil NH_4^+-N concentration generally increased with elevation, whilst NO_3^--N and AP did not vary significantly between zones. DOC concentration increased with elevation, reaching a mean of 109.4 mg kg^{-1} at AM, double that in the EB and coniferous and broad-leaved mixed forest (CB) vegetation zones. Soil TN and TC concentrations also increased significantly with elevation, although the C/N ratio remained relatively constant. In general, the MNC index increased with elevation (Table 1).

An UpSet plot were used to visualize the common-shared, partial-shared, and unique DOM molecules for the five vegetation zones along the elevation gradients in the Wuyi Mountains (Fig. S1). The number of detected molecular formulae of soil DOM at the five different vegetation zones ascending with altitude from evergreen broad-leaved forest (EB) to AM was 1168, 3106, 1206, 3392, and 2325, respectively. The common shared molecules (present in all five samples) accounted for the largest proportion from the intersection of different vegetation zones. Inter sample rankings analysis was performed to reveal possible differences in quality in the 703 common DOM components present in the five vegetation zones (Fig. 1). DOM qualities differed considerably across the vegetation zones at different elevations. At the EB site, DOM molecular formulae ranked 1 (relatively high peak intensities) exhibited H/C > 0.9 and O/C ≤ 0.5, whilst those ranked 4 and 5 mainly had O/C > 0.5. In contrast, at sites DF and AM, DOM formulae ranked 4 and 5 mainly exhibited H/C > 1 and O/C ≤ 0.55. The DOM molecular formulae ranked 1 at site AM were dominated by H/C < 1, whilst formulae ranked 1 and 2 at DF displayed high m/z values (> 400) with O/C > 0.5. Unique DOM molecular formulae at DF and AM were dominated by tannin- and aromatic structures- like compounds, respectively (Fig. S2).

Lignins/CRAM-like (carboxylic rich alicyclic molecule) structures dominated soil DOM composition in all vegetation zones, and its abundance decreased with increasing elevation (Fig. S3). The relative abundance of aliphatic/proteins and lipids also decreased with elevation, whilst those of tannin and aromatic structures increased with elevation (Fig. S3d). The weighted mean

10

289 O/C ratio, AI_{mod}, and NOSC values of DOM molecules showed increasing trends with elevation,

290 whilst the H/C ratio and molecular lability boundary (MLB_L) percentage decreased (Table 2). The

291 Shannon index values of DOM molecules in the coniferous forest (CF) were slightly lower than in

292 the other vegetation zones (Table 2). This is consistent with the narrower ranges of the distribution

293 curves for the number of C and O atoms and M/Z values of DOM compositions in CF compared

294 to the other vegetation zones (Fig. S3).

295

3.2. Soil microbial diversity, community structure and assembly processes along the elevation

gradient

298 Within the soil bacterial community, *Acidobacteria* (36.2%–42.6%), *Proteobacteria* (24.5%–

299 32.3%), *Chloroflexi* (7.51%–14.2%), *Actinobacteria* (5.97%–8.4%) and *Planctomycetes* (2.14%–

300 5.77%) were the five most abundant phyla in all five vegetation types (numbers in parentheses are

301 minimum and maximum values of mean % abundance amongst the different sites, Fig. S4a). They

302 displayed no clear trend in abundance with elevation, although the relative abundance of

303 *Verrucomicrobia* (0.99%–2.69%) decreased with elevation (Fig. S3b). In the fungal community,

304 *Basidiomycota* (53.7%–82.5%) dominated at all sites. Its relative abundance was highest at the

305 lowest elevation in the evergreen broad-leaved forest (EB) zone, and then decreased before

306 increasing with elevation. The relative abundance of *Mortierellomycota* phylum also generally

307 increased with elevation (Fig. S4c).

308 The Chao1 index and Faith's PD index of soil bacteria decreased with increasing elevation (Fig.

309 S5a and Fig. S6a), whilst the indices for fungi were not significantly different between elevations

310 (Fig. S5d and Fig. S6b). The Shannon indices for both the bacterial and fungal communities

311 increased from EB to the coniferous and broad-leaved mixed forest (CB) zone and then showed a

312 decreasing trend with elevation (Fig. S5b, e). Non-metric multidimensional scaling (NMDS)

313 analysis showed that the soil bacterial and fungal communities at the different sites formed distinct

314 clusters, which are completely separate in the ordination space (Anosim test, Global R = 1, *P* <

315 0.001) (Fig. S5c, f). Beta diversity, estimated among the microbial communities in all 15 soil

316 samples based on Bray-Curtis dissimilarities, was significantly lower among bacteria than fungi

317 (Fig. S7).

11

318   The potential linkages among soil bacteria and fungi OTUs were revealed by the co-occurring

319   network analysis (Fig. 2a, b). Compared with the Erdös-Réyni random network, a higher clustering

320   coefficient and average path length were observed in the co-occurrence networks of bacterial and

321   fungal communities (Fig. 2a, b). This displayed that the generated networks were more clustered

322   than the identically sized random networks and that their degree distributions are non-random. The

323   modularity and average path length of the fungal community were greater than for the bacterial

324   network. In the fungal community most connections were positive (93%), in contrast to the bacterial

325   community where only 55% of connections were positive.

326   Neutral processes dominated assembly of the bacterial and fungal communities overall along

327   the elevation gradient, with 72.9% and 56.6% of the community variation explained by the neutral

328   community model (NCM), respectively (Fig. 2c, d). The values of m (migration rate) were 0.561

329   and 0.123 for the bacterial and fungal community, respectively (Fig. 2c, d). To detect the relative

330   importance of stochastic and deterministic processes in the assembly of the bacterial and fungal

331   communities at different elevations, we calculated the modified stochasticity ratio (MST) in each

332   vegetation zone (Fig. 2e). The MST value for the fungal community in CB was significantly higher

333   than in other vegetation zones. In addition, MST values were < 0.5 for both bacteria and fungi in the

334   AM zone.

335

336   **3.3. Correlation between soil chemical properties, DOM components, and microbial**

337   **community characteristics**

338   Correlation analysis across all elevations revealed that the Chao 1 index for the bacterial community

339   was significantly negatively correlated with tannins, aromatic structures, and the AI_{mod} value of

340   DOM compounds (Fig. 3a). Conversely, lignins/CRAM-like structures and aliphatic/proteins

341   components were significantly positively correlated with the bacterial Chao1 index (Fig. 3a). The

342   relative abundance of lignins/CRAM-like structures and aliphatic/proteins compounds were

343   significantly negatively correlated with soil TC、NH_4^+-N, and TN contents ($P < 0.05$). However,

344   the relative abundance of tannins was significantly positively correlated with soil TN and TC

345   contents (Fig. S8).

346   Highly significant correlations ($P < 0.01$) between the 100 most abundant DOM molecular

12

formulae and bacteria and fungi OTUs at the phylum level were selected to construct network diagrams. For bacteria (Fig. 3b), formulae of lignins/CRAM-like structures were positively correlated with most microbes, whilst *Chloroflexi* was negatively correlated with some tannin molecules. *Proteobacteria* was only positively correlated with individual DOM molecules, whilst *Chloroflexi* only had negative correlations. The number of C atoms in DOM formulae correlated with *Proteobacteria* had a small range of 15–21, while those correlated with *Acidobacteria* had a relatively large range of 13–23. For fungi (Fig. 3c), there were a smaller number of correlations between phyla and individual DOM molecules, and all correlations were positive and with lignins/CRAM-like structures, apart from one formula. More DOM molecular formulae were correlated with *Ascomycota* than with *Basidiomycota*.

3.4. Microbial drivers of soil multi-nutrient cycling

We applied random forest (RF) analysis to identify the major potential microbial drivers of soil multiple nutrient cycling across all sites. Site elevation, alpha diversity (PD whole tree and Chao1 indices), and the relative abundance of *Verrucomicrobia* and *Firmicutes* were the most important bacterial community indicators of the soil multi-nutrient cycling (MNC) index (Fig. 4a). The significant fungal community predictors were site elevation, relative abundance of three fungal phyla, and the alpha diversity (PD whole tree and Shannon indices). Partial least squares path models (PLS-PM) analyzed the effects of microbial community characteristics on the soil MNC index, which had best fit goodness-of-fit (GOF) values of > 0.70 for microbial communities (Fig. 4c). The PLS-PM also highlighted the strong direct effects of elevation on soil microbial community diversity, although the effects are in opposite directions: high elevation has a negative effect on the bacterial alpha diversity index (path coefficient = -0.91, $P < 0.001$) but a positive effect on the fungal alpha diversity index (path coefficient = 0.59, $P < 0.05$). The Shannon diversity index of fungal community exhibited direct negative effects on MNC (path coefficient = -0.56, $P < 0.05$).

4. Discussion

4.1. Refractory components of soil DOM molecules gradually increase along the elevation

376 **gradient**

377 In our study elevation transect in the Wuyi Mountains, the MLB_L (%) decreased and AI_{mod} and

378 NOSC values of DOM molecules increased with elevation. Since higher AI_{mod} and NOSC values

379 indicate greater recalcitrance (low bioavailability) of DOM compounds (Cai and Jiao, 2023; Hu et

380 al., 2022), this indicates that soil DOM resistance increased with elevation. The DBE and O/C ratio

381 of soil DOM molecules increased along our study elevation gradient (Table 2), which is consistent

382 with the elevational variation in DOM components in restored areas of the Loess Plateau (Hu et al.,

383 2021), but contrasts with results in the higher altitude Sygera Mountains on the Tibetan Plateau

384 (Zhang et al., 2022). The DBE value reflects the degree of unsaturation of the DOM molecules

385 (Melendez-Perez et al., 2016), with higher values indicating greater unsaturation and lower

386 bioavailability (Cai and Jiao, 2023). Ligand exchange between the carboxyl / hydroxyl functional

387 groups of the DOM compounds and the surface of Fe oxides is the main mechanism of adsorption of

388 soil DOM molecules (Ding, 2020). An experimental study demonstrated that adsorption of the more

389 oxidized DOM components increased at low DOM concentrations, whilst at high DOM

390 concentrations selective adsorption of the less oxidized DOM components occurred (Avneri-Katz et

391 al., 2017). These processes appear to occur along our study elevation transect, with more oxidized

392 DOM components remaining in the soil liquid phase at the high-elevation sites. In contrast, at the

393 lower elevation sites, the oxidized DOM components were more readily adsorbed at soil solid phase

394 surfaces (and not extracted for analysis in our ultrapure water extraction (Bahureksa et al., 2021)),

395 thus decreasing the C accessibility for microbial degradation. Soil iron-containing minerals retain

396 great quantities of SOM (Lv et al., 2017). Highly oxidized and more aromatic DOM molecules are

397 preferentially adsorbed on hematite surfaces (Lv et al., 2017), and preferential adsorption of high

398 molar mass organic solutes occurs on goethite surfaces (Liu et al., 2014). The soil in the Wuyi

399 Mountains is highly leached, with mineral composition dominated by hematite in low-elevation red

400 earth soils and goethite at higher elevations in yellow earth soils (Lin, 2010). Soil mineralogy,

401 therefore, helps explain the lower molar mass (M/Z) and O/C values of the DOC molecules

402 extracted at the lowest elevation EB site.

403 The abundances of DOM molecules with lipids- and aliphatic/proteins-like compositions

404 decreased with increasing elevation on our study transect. Conversely, aromatic- and tannin- like

compounds increased, indicating DOM compounds derived from microbe to plants along the elevation gradient (Shen et al., 2023). Tannins are secondary metabolites of polyphenols produced by higher plants, which can leach from litter into soil, and are toxic to microbial metabolism and can inhibit enzyme activity, thereby affecting nutrient cycling (Triebwasser et al., 2012; Kraus et al., 2003). Feng et al. (2021) showed that soil microbial metabolic efficiency decreased with elevation, which was attributed partly to the microbial community increasing investment in nutrient acquisition via enzymes. Thereby, the decrease with elevation of microbial-derived DOM along our elevation transect is attributed to the expected inhibition of microbial activity. We also found that the relative abundance of lignin/CRAM-like structure compounds decreased with increasing altitude. Lignins in soil are mainly generated from above-ground and subsurface (root) litter of higher plants, though biotic, aerobic and co-metabolic degradation processes (Thevenot et al., 2010). For example, white rot fungi of *Basidiomycetes* secrete ligninolytic enzymes, which can convert and mineralize refractory DOM into CO_2 and water by co-metabolizing aliphatic and aromatic substances (Agrawal et al., 2021). The change of lignin input source during the transition from trees to graminaceous plants and the strong degradation of saprophytic fungi at higher elevation may explain the change of lignin-like compounds to some extent along the study transect.

Interestingly, the DOM molecules in soil from the coniferous forest (CF) site had a narrower range of number of C and O atoms and M/Z values (Fig. S3), which is consistent with the results of Li et al. (2021) for soil DOM of monoculture Chinese fir (*Cunninghamia lanceolata* (Lamb.) Hook.) plantations. Soil DOM provides carbon-containing substrates for the soil microbial community, and the latter affects DOM composition by supplying metabolites and residues (Wu M. et al., 2021). Plant litter is an important main source of soil DOC (Don and Kalbitz, 2005). Therefore, differences in litter-fall and the metabolites and residues of microorganisms in vegetation zones along elevation gradients may be one important cause of changes in DOM molecular composition. For instance, the low input of soil nutrients from litter-fall (Ma et al., 2007) may partly explain the soil DOM variation in Chinese fir plantations of different ages.

The van Krevelen diagram is widely used for visualization of DOM molecular types and

434　characteristics, and identification of possible chemical reactions (Kim et al., 2003). Nevertheless,

435　it is important to note that the molecular composition (molecular formulae) only of DOM is

436　obtained based on FT-ICR MS but not the isomer features (Hu et al., 2022). It is therefore

437　necessary in future studies to identify the structural features of DOM molecules to reveal their full

438　role in soil ecosystems (Qi et al., 2022).

439

440　**4.2. Deterministic processes dominate the low-diversity microbial assembly at high elevation**

441　The MST values of the soil bacteria and fungi communities were below the 0.5 threshold in the

442　alpine meadow zone, indicating that deterministic processes dominate microbial assembly at the

443　highest elevation site (Fig. 2e). Furthermore, the microbial community at this site had low Shannon

444　diversity indices compared to many of the lower elevation vegetation zones (Fig. S5b, e).

445　Environmental filters, including temperature, precipitation, soil available nutrient contents and

446　physical properties, and vegetation types can select for microbial species with specific traits, such as

447　stress tolerances and nutrient acquisition (Anthony et al., 2020). Such effects have been reported in

448　a number of studies. For instance, microbial community diversity and enzyme activity were

449　affected more by changing climatic factors, such as mean annual temperature and precipitation,

450　than soil characteristics along an elevation gradient on Taibai Mountain in eastern China (Ren et

451　al., 2020). Mo et al. (2021) reported that deterministic processes influenced the microeukaryotic

452　plankton community assembly with narrow habitat niche breadths under high salinity conditions.

453　Furthermore, Xun et al. (2019) indicated that environmental selection increased in low-diversity

454　bacterial communities, which contributed to the dominance of deterministic processes. Reduced soil

455　temperature and increased soil moisture were observed with elevation in the Wuyi Mountains

456　related to lower air temperature and elevated precipitation (Table S1), which results in slower

457　decomposition rates of SOM at high elevation (Bu et al., 2012). Collectively, increasing

458　environmental and physiological stress on microorganisms along the elevation gradient (Ren et al.,

459　2020), including the reduced abundance of labile DOM (H/C $\geq$ 1.5), high C/N ratio substrates

460　(Anthony et al., 2020) and increasing abundance of tannins, are suggested to lead to the dominance

461　of deterministic assembly processes for the microbial community at the highest elevation site in the

462　Wuyi Mountains.

Co-occurring network analysis is a useful method for identifying potential microbial interactions and functional distribution (Chen W. J. et al., 2021). The results of co-occurring network analysis showed that positive associations were more dominant among the fungal community than the bacterial community at the study sites (Fig. 2a, b), suggesting possible niche overlap and mutualistic or facilitative interactions between the fungal species (Zhu et al., 2021). The lower average path length and higher average degree of the bacterial co-occurring network indicates closer relationships among the OTUs and rapid distribution of any perturbation (Li et al., 2020; Yuan et al., 2021).

The emergence and maintenance of soil microbial diversity are underpinned by soil heterogeneity (Nunan et al., 2020). In this study, soil fungal communities had higher beta diversity than bacterial communities (Fig. S7) which is consistent with the results of Jiao et al. (2018). The bacterial community across all sites had lower path length, lower dispersal limitation (lower m value), and wider habitat niche breadths than fungal taxa (Fig. 2a, c, d and Fig. S9), which have a smaller body size and more flexible metabolic plasticity, and therefore are less environmentally filtered (Wu W. X. et al., 2018). The interaction between disturbance and dispersal can homogenize species composition, which was observed to cause decreased beta diversity (Catano et al., 2017). The relative proportions of soil heterotrophic microorganisms are determined by the local geographic environment, vegetation types, and soil factors (Zhuang et al., 1997). For example, Li et al. (2021) found that the soil fungal Faith's PD index declined with elevation in the cold temperate zone at high latitudes in China. Microbial diversity positively regulates the service functions of terrestrial ecosystems by changing the nutrient supply and distribution of terrestrial ecosystems (Delgado-Baquerizo et al., 2016).

Overall, in this study, the Chao 1 and Faith's PD diversity indexes of bacterial communities decreased along a subtropical elevation gradient (Fig. S5a and Fig. S6a). Ma et al. (2022) also reported that the bacteria community richness index and Faith's PD index decreased with elevation in subtropical forests, with soil temperature largely explaining the changes in soil bacterial and fungal diversity. Bacterial community diversity largely drives the utilization efficiency of C (Domeignoz-Horta et al., 2020). Reduced abundance of labile DOM (H/C $\geq$ 1.5) and increasing abundance of tannins may reduce soil enzyme activity, thereby reducing bacterial community

17

492   diversity.

493   Microbial life history strategies also influence soil DOM composition. For example, Zeng et al.

494   (2022) found that microbial assemblies shifted from using labile to recalcitrant carbon with

495   increasing elevation. In our study, *Chloroflexi* had higher relative abundance at the highest

496   elevation AM site (Fig. S4a) and also its abundance was negatively correlated with

497   lignins/CRAM-like structures and tannins in DOM molecules (Fig. 3b). Positive correlations

498   between microbial compositions and DOM molecules are indicative of the generation of new

499   molecules by microbial activity, whilst negative correlations are interpreted as the decomposition

500   of DOM molecules based on resource-consumer relationships (Hu et al., 2022). *Chloroflexi* can

501   decompose recalcitrant C-containing components and are considered a *K*-selected microbe

502   (Adamczyk et al., 2021). Combined with our study results, this suggests the selection of substrates

503   with low bioavailability by *Chloroflexi*.

504

505   **4.3. Bacteria drive the degradation of labile soil DOM components, and the fungal**

506   **community is the key control on soil nutrient cycling**

507   The soil bacterial community contained a slightly higher percentage of habitat generalists and had

508   a larger niche breadth compared to the fungal community, which had a higher percentage of

509   habitat specialists (Fig. S9), indicating that the soil bacterial community had more competitive

510   ability than the fungi. Highly labile substrates, for which bacterial communities have a high affinity

511   (Osterholz et al., 2016), can reach steady-state equilibrium concentrations below detection limits.

512   The significant correlations across the study sites between the Chao1 index for bacteria and the H/C

513   and O/C ratios of DOM components (positive and negative, respectively) (Fig. 3a), indicate that the

514   bacterial community plays an important role in the degradation of labile components. The Chao1

515   index of the bacterial community was also significantly positively correlated with soil DOM

516   aliphatic/protein compounds, concurring with other studies reporting positive associations between

517   bacterial abundance and activity and aliphatic DOM components (Kamjunke et al., 2019). From the

518   results of the FAPROTAX database functional annotation, we found that bacterial OTUs with

519   functional photoheterotrophy increased with elevation, whilst those with functional nitrification

520   and aerobic nitrite oxidation decreased overall with altitude (Fig. S10). Furthermore, the soil MNC

521 index increased along the altitude gradient (Table 1). Thus, changes in microbial investment in

522 nutrient acquisition may lead to this interaction between soil nutrients and microbial communities.

523   Fungal extracellular polymeric substances and hyphae networks are conducive to the

524 transmission and aggregation of plant-derived litter derivatives to increase the decomposition

525 efficiency and persistence of SOM (De Beeck et al., 2021; Witzgall et al., 2021). Fungi are

526 regarded as oligotrophs, exhibiting effective degradation of refractory carbon substrates (Ho et al.,

527 2017). The soil fungal community plays a vital role in nutrient cycling and organic matter

528 transformation, such that fungal community structure and biomass provide an early indicator of soil

529 environmental changes (Wu et al., 2019). Specifically, the relative abundance of the fungal phylum

530 *Mortierellomycota* increased with elevation and was significantly positively correlated with soil AK

531 and DOC concentrations (Fig. S4c and S11a). *Mortierellomycota* are *r*-selected saprotrophic

532 microorganisms that have a low life expectancy and stronger growth in environments with high

533 available resources and low-stress exposure (Wu et al., 2021).

534   In contrast, the relative abundance of the bacterial phylum *Verrucomicrobia* was significantly

535 negatively correlated with soil NH_4^+-N, AK, and DOC concentrations (Fig. S11b, c), and with

536 tannin abundance (Fig. S12). This is interpreted as indicative of the oligotrophic lifestyle of

537 *Verrucomicrobia* (Navarrete et al., 2015). In our study, the relative abundance of tannins were

538 significantly positively correlated with soil TC and TN concentrations (Fig. S8), which showed

539 that tannins was beneficial to the sequestration of carbon and nitrogen. The dominant fungal

540 phylum *Basidiomycota* in our study had the highest relative abundance in the lowest elevation

541 vegetation zone EB, and then decreased, followed by an increasing trend with elevation from CB to

542 AM (Fig. S4c). *Basidiomycota* are representative of oligotrophic fungi, which can degrade

543 refractory compounds, and were found to be most abundant in warmer soil conditions along a

544 temperate forest transect characterized by a K-strategy fungal community (Li et al., 2021). Thus the

545 increase in the relative abundance of *Basidiomycota* with elevation in our study can partly explain

546 the shift to K strategy due to the refractory components (H/C < 1.5) of soil DOM with elevation.

547

548 **5. Conclusions**

549 It is well-known that the soil microbial community has a profound impact on DOM composition and

multi-nutrient cycling in ecosystems. Changes in the functional group of soil bacterial community with elevation, related to investment in nutrient acquisition, may account for changes in soil nutrient cycling. Neutral processes dominated overall the bacterial and fungal communities assembly along the elevation transect, and bacteria have a higher niche breadth and lower dispersal limitation than fungi. However, deterministic selection dominated the microbial community assembly at the highest elevation site, which may be attributed to the reduced soil temperature and increased soil moisture, and increased relative abundance of tannin and aromatic structures in soil DOM. This increased abundance of potentially resistant DOM components could be interpreted as enhanced soil carbon sequestration capacity with increasing elevation, but their stability is not assured if vegetation zones at lower elevations with higher rates of DOM degradation move upwards in response to climate warming. As a relatively active fraction of the soil C pool, DOM molecules are greatly affected by microbial community, and anthropogenic-driven climate change increases the possibility of DOM degradation. Since sampling was conducted in winter, care should be taken in interpreting the interconnection between soil DOM components and microorganisms in the Wuyi Mountains in other seasons.

References

Abatenh, E., Gizaw, B., Tsegaye, Z., Tefera, G., 2018. Microbial Function on Climate Change - A Review. Open Journal of Environmental Biology 3(1), 1-7. https://doi.org/10.17352/ojeb.000008.

Adamczyk, M., Rüthi, J., Frey, B., 2021. Root exudates increase soil respiration and alter microbial community structure in alpine permafrost and active layer soils. Environmental Microbiology 23(4), 2152-2168. https://doi.org/10.1111/1462-2920.15383.

Agrawal, N., Barapatre, A., Shahi, M.P., Shahi, S.K., 2021. Biodegradation Pathway of Polycyclic Aromatic Hydrocarbons by Ligninolytic Fungus *Podoscypha elegans* Strain FTG4 and Phytotoxicity Evaluation of their Metabolites. Environmental Processes 8(3), 1307-1335. https://doi.org/10.1007/s40710-021-00525-z.

Anthony, M. A., Crowther, T. W., Maynard, D. S., van den Hoogen, J., Averill, C., 2020. Distinct

579   Assembly Processes and Microbial Communities Constrain Soil Organic Carbon Formation.

580   One Earth 2(4), 349-360. https://doi.org/10.1016/j.oneear.2020.03.006.

581 Avneri-Katz, S., Young, R. B., McKenna, A. M., Chen, H., Corilo, Y. E., Polubesova, T., Borch, T.,

582   Chefetz, B., 2017. Adsorptive fractionation of dissolved organic matter (DOM) by mineral soil:

583   Macroscale approach and molecular insight. Organic Geochemistry 103, 113-124.

584   https://doi.org/10.1016/j.orggeochem.2016.11.004.

585 Bae, E. J., Yeo, I. J., Jeong, B., Shin, Y., Shin, K. H., Kim, S., 2011. Study of double bond

586   equivalents and the numbers of carbon and oxygen atom distribution of dissolved organic

587   matter with negative-mode FT-ICR MS. Analytical Chemistry 83(11), 4193-4199.

588   https://doi.org/10.1021/ac200464q

589 Bahureksa, W., Tfaily, M. M., Boiteau, R. M., Young, R. B., Logan, M. N., McKenna, A. M., Borch,

590   T., 2021. Soil Organic Matter Characterization by Fourier Transform Ion Cyclotron Resonance

591   Mass Spectrometry (FTICR MS): A Critical Review of Sample Preparation, Analysis, and

592   Data Interpretation. Environmental Science & Technology 55(14), 9637-9656.

593   https://doi.org/10.1021/acs.est.1c01135.

594 Bu, X. L., Ding, J. M., Wang, L. M., Yu, X. N., Huang, W., Ruan, H. H., 2011. Biodegradation and

595   chemical characteristics of hot-water extractable organic matter from soils under four different

596   vegetation types in the Wuyi Mountains, southeastern China. European Journal of Soil Biology

597   47(2), 102-107. https://doi.org/10.1016/j.ejsobi.2010.11.009.

598 Bu, X. L., Ruan, H. H., Wang, L. M., Ma, W. B., Ding, J. M., Yu, X. N., 2012. Soil organic matter in

599   density fractions as related to vegetation changes along an altitude gradient in the Wuyi

600   Mountains, southeastern China. Applied Soil Ecology 52, 42-47.

601   https://doi.org/10.1016/j.apsoil.2011.10.005.

602 Byrnes, J. E. K., Gamfeldt, L., Isbell, F., Lefcheck, J. S., Griffin, J. N., Hector, A., Cardinale, B. J.,

603   Hooper, D. U., Dee, L. E., Duffy, J. E., 2014. Investigating the relationship between

604   biodiversity and ecosystem multifunctionality: challenges and solutions. Methods in Ecology

605   and Evolution, 5(2), 111-124. https://doi.org/10.1111/2041-210X.12143.

606 Cai, R. H., Jiao, N. Z. 2023. Recalcitrant dissolved organic matter and its major production and

607   removal processes in the ocean. Deep Sea Research Part I: Oceanographic Research Papers,

191, 103922. https://doi.org/10.1016/j.dsr.2022.103922.

Cao, C., Ruan, C. Y., Ren, Y. B., Zhang, S. L., Xiong, X. L., Li, X. J., Lyu, M. K., Xie, J. S., 2020. Effects of stimulating warming on surface soil carbon, nitrogen and its enzyme activities across a subtropical elevation gradient in Wuyi Mountain, China. Acta Ecologica Sinica 40(15), 5347-5356. (in Chinese).

Catano, C. P., Dickson, T. L., Myers, J. A., 2017. Dispersal and neutral sampling mediate contingent effects of disturbance on plant beta-diversity: a meta-analysis. Ecology Letters 20(3), 347-356. https://doi.org/10.1111/ele.12733.

Chen, Q. L., Hu, H. W., Yan, Z. Z., Li, C. Y., Nguyen, BA. T., Sun, A. Q., Zhu, Y. G., He, J. Z., 2021. Deterministic selection dominates microbial community assembly in termite mounds. Soil Biology & Biochemistry 152, 108073. https://doi.org/10.1016/j.soilbio.2020.108073.

Chen, W. D., Ren, K. X., Isabwe, A., Chen, H. H., Liu, M., Yang, J., 2019. Stochastic processes shape microeukaryotic community assembly in a subtropical river across wet and dry seasons. Microbiome 7, 148. https://doi.org/10.1186/s40168-019-0749-8.

Chen, W. J., Zhou, H. K., Wu, Y., Li, Y. Z., Qiao, L. L., Wang, J., Zhai, J. Y., Song, Y. H., Zhao, Z. W., Zhang, Z. H., Liu, G. B., Zhao, X. Q., You, Q. M., Xue, S., 2021. Plant-mediated effects of long-term warming on soil microorganisms on the Qinghai-Tibet Plateau. Catena 204, 105391. https://doi.org/10.1016/j.catena.2021.105391.

Dai, Z. M., Zang, H. D., Chen, J., Fu, Y. Y., Wang, X. H., Liu, H. T., Shen, C. C., Wang, J. J., Kuzyakov, Y., Becker, J. N., Hemp, A., Barberán, A., Gunina, A., Chen, H. H., Luo, Y., Xu, J. M., 2021. Metagenomic insights into soil microbial communities involved in carbon cycling along an elevation climosequences. Environmental Microbiology 23(8), 4631-4645. https://doi.org/10.1111/1462-2920.15655.

De Beeck, M. O., Persson, P., Tunlid, A., 2021. Fungal extracellular polymeric substance matrices – Highly specialized microenvironments that allow fungi to control soil organic matter decomposition reactions. Soil Biology and Biochemistry 159, 108304. https://doi.org/10.1016/j.soilbio.2021.108304.

Delgado-Baquerizo, M., Maestre, F. T., Reich, P. B., Jeffries, T. C., Gaitan, J. J., Encinar, D., Berdugo, M., Campbell, C. D., Singh, B. K., 2016. Microbial diversity drives

multifunctionality in terrestrial ecosystems. Nature Communications 7, 10541. https://doi.org/10.1038/ncomms10541.

de Mendiburu, F. (2021). Package `agricolae': Statistical Procedures for Agricultural Research. R package v1.3-5. https://CRAN.R-project.org/package=agricolae.

Domeignoz-Horta, L. A., Pold, G., Liu, X.-J. A., Frey, S. D., Melillo, J. M., DeAngelis, K. M., 2020. Microbial diversity drives carbon use efficiency in a model soil. Nature Communications 11, 3684. https://doi.org/10.1038/s41467-020-17502-z.

Don, A., Kalbitz, K., 2005. Amounts and degradability of dissolved organic carbon from foliar litter at different decomposition stages. Soil Biology and Biochemistry, 37(12), 2171-2179. https://doi.org/10.1016/j.soilbio.2005.03.019.

Dove, N. C., Torn, M. S., Hart, S. C., Taş, N., 2021. Metabolic capabilities mute positive response to direct and indirect impacts of warming throughout the soil profile. Nature Communications 12, 2089. https://doi.org/10.1038/s41467-021-22408-5.

Feng, J., Zeng, X. M., Zhang, Q. G., Zhou, X. Q., Liu, Y. R., Huang, Q. Y., 2021. Soil microbial trait-based strategies drive metabolic efficiency along an altitude gradient. IS ME Communication, 1, 71. https://doi.org/10.1038/s43705-021-00076-2.

Fouché, J., Christiansen, C. T., Lafrenière, M. J., Grogan, P., Lamoureux, S. F., 2020. Canadian permafrost stores large pools of ammonium and optically distinct dissolved organic matter. Nature Communications 11, 4500. https://doi.org/10.1038/s41467-020-18331-w.

Gao, X. F., Chen, H. H., Gu, B. H., Jeppesen, E., Xue, Y. Y., Yang, J., 2021. Particulate organic matter as causative factor to eutrophication of subtropical deep freshwater: Role of typhoon (tropical cyclone) in the nutrient cycling. Water Research 188, 116470. https://doi.org/10.1016/j.watres.2020.116470.

Gougoulias, C., Clark, J. M., Shaw, L. J., 2014. The role of soil microbes in the global carbon cycle: tracking the below-ground microbial processing of plant-derived carbon for manipulating carbon dynamics in agricultural systems. Journal of the Science of Food and Agriculture 94(12), 2362-2371. https://doi.org/10.1002/jsfa.6577.

He, R., Wang, G. B., Wang, J. S., Xu, B. F., Wang, K. J., Fang, Y. H., Shi, Z., Ruan, H. H., 2009. Seasonal variation and its main affecting factors of soil microbial biomass under different

666 vegetations along an elevation gradient in Wuyi Mountains of China. Chinese Journal of
667 Ecology, 28(3), 394-399. (in Chinese).

668 Ho, A., Di Lonardo, D. P., Bodelier, P. L. E., 2017. Revisiting life strategy concepts in
669 environmental microbial ecology. FEMS Microbiology Ecology 93(3), fix006.
670 https://doi.org/10.1093/femsec/fix006.

671 Hu, A., Choi, M., Tanentzap, A. J., Liu, J. F. Jang, K. S., Lennon, J. T., Liu, Y. Q., Soininen, J., Lu,
672 X. C., Zhang, Y. L., 2022. Ecological networks of dissolved organic matter and
673 microorganisms under global change. Nature Communications, 13(1), 3600.
674 https://doi.org/10.1038/s41467-022-31251-1.

675 Hu, H. Y., Umbreen, S., Zhang, Y. L., Bao, M. Z., Huang, C. F., Zhou, C. F., 2021. Significant
676 association between soil dissolved organic matter and soil microbial communities following
677 vegetation restoration in the Loess Plateau. Ecological Engineering, 169, 106305.
678 https://doi.org/10.1016/j.ecoleng.2021.106305.

679 Huang, W., McDowell, W. H., Zou, X. M., Ruan, H. H.,Wang, J. S., Ma, Z. L., 2015. Qualitative
680 differences in headwater stream dissolved organic matter and riparian water-extractable soil
681 organic matter under four different vegetation types along an altitudinal gradient in the Wuyi
682 Mountains of China. Applied Geochemistry 52, 67-75.
683 https://doi.org/10.1016/j.apgeochem.2014.11.014.

684 Jiao, S., Liu, Z. S., Lin, Y. B., Yang, J., Chen, W. M., Wei, G. H., 2016. Bacterial communities in
685 oil contaminated soils: Biogeography and co-occurrence patterns. Soil Biology and
686 Biochemistry 98, 64-73. https://doi.org/10.1016/j.soilbio.2016.04.005.

687 Jiao, S., Chen, W. M., Wang, J. L., Du, N. N., Li, Q. P., Wei, G. H., 2018. Soil microbiomes with
688 distinct assemblies through vertical soil profiles drive the cycling of multiple nutrients in
689 reforested ecosystems. Microbiome 6, 146. https://doi.org/10.1186/s40168-018-0526-0.

690 Jiao, S., Peng, Z. H., Qi, J. J., Gao, J. M., Wei, G. H., 2021. Linking Bacterial-Fungal Relationships
691 to Microbial Diversity and Soil Nutrient Cycling. mSystems 6(2), e01052-20.
692 https://doi.org/10.1128/mSystems.01052-20.

693 Kamjunke, N., Hertkorn, N., Harir, M., Schmitt-Kopplin, P., Griebler, C., Brauns, M., von
694 Tümpling, W., Weitere, M., Herzsprung, P., 2019. Molecular change of dissolved organic

695 matter and patterns of bacterial activity in a stream along a land-use gradient. Water Research

696 164, 114919. https://doi.org/10.1016/j.watres.2019.114919.

697 Kim, S., Kramer, R. W., Hatcher, P. G., 2003. Graphical method for analysis of ultrahigh-resolution

698 broadband mass spectra of natural organic matter, the van Krevelen diagram. Analytical

699 Chemistry, 75(20), 5336-5344. https://doi.org/10.1021/ac034415p.

700 Kraus, T. E. C., Dahlgren, R. A., Zasoski, R. J., 2003. Tannins in nutrient dynamics of forest

701 ecosystems - a review. Plant and Soil 256(1), 41-66.

702 https://doi.org/10.1023/A:1026206511084.

703 Körner, C., 2007. The use of 'altitude' in ecological research. Trends in Ecology & Evolution 22(11),

704 569-574. https://doi.org/10.1016/j.tree.2007.09.006.

705 Koven, C. D., Ringeval, B., Friedlingstein, P., Ciais, P., Cadule, P., Khvorostyanov, D., Krinner, G.,

706 Tarnocai, C., 2011. Permafrost carbon-climate feedbacks accelerate global warming.

707 Proceedings of the National Academy of Sciences of the United States of America 108(36),

708 14769-14774. https://doi.org/10.1073/pnas.1103910108.

709 Li, J. B., Li, C. N., Kou, Y. P., Yao, M. J., He, Z. L., Li, X. Z., 2020. Distinct mechanisms shape soil

710 bacterial and fungal co-occurrence networks in a mountain ecosystem. FEMS Microbiology

711 Ecology 96(4), fiaa030. https://doi.org/10.1093/femsec/fiaa030.

712 Li, H., Yang, S., Semenov, M. V., Yao, F., Ye J., Bu, R. C., Ma, R. A., Lin, J. J., Kurganova, I., Wang,

713 X. G., Deng, Y., Kravchenko, I., Jiang, Y., Kuzyakov, Y., 2021. Temperature sensitivity of

714 SOM decomposition is linked with a K-selected microbial community. Global Change Biology

715 27(12), 2763-2779. https://doi.org/10.1111/gcb.15593.

716 Li, J., Yang, Y. C., Yang, L. X., 2021. Seasonal variations in soil fungal communities and

717 co-occurrence networks along an altitudinal gradient in the cold temperate zone of China: A

718 case study on Oakley Mountain. Catena 204, 105448.

719 https://doi.org/10.1016/j.catena.2021.105448.

720 Li, X. M., Chen, Q. L., He, C., Shi, Q., Chen, S. C., Reid, B. J., Zhu, Y. G., Sun, G. X., 2019.

721 Organic Carbon Amendments Affect the Chemodiversity of Soil Dissolved Organic Matter

722 and Its Associations with Soil Microbial Communities. Environmental Science & Technology

723 53(1), 50-59. https://doi.org/10.1021/acs.est.8b04673.

724   Liang, C., Amelung, W., Lehmann, J., Kästner, M., 2019. Quantitative assessment of microbial

725   necromass contribution to soil organic matter. Global Change Biology 25(11), 3578-3590.

726   https://doi.org/10.1111/gcb.14781.

727   Lin, L. Q., 2010. The Vertical Distribution of Iron Oxide in Wuyi Mountain and Its Causes Analysis.

728   Hunan Agricultural Sciences 17, 70-71+75. (in Chinese).

729   Liu, H., Liu, X., Li, X., Fu, Z., Lian, B., 2021. The molecular regulatory mechanisms of the bacteria

730   involved in serpentine weathering coupled with carbonation. Chemical Geology 565, 120069.

731   https://doi.org/10.1016/j.chemgeo.2021.120069.

732   Liu, H. B., Chen, T. H., Frost R. L., 2014. An overview of the role of goethite surfaces in the

733   environment. Chemosphere 103, 1-11. https://doi.org/10.1016/j.chemosphere.2013.11.065.

734   Liu, Y., Li, J., Sun, H., Chen, Y. W., Li, X., 2020. Stability of soil organic carbon along the

735   altitudinal gradient in alpine of the west of Sichuan Province. Research of Soil and Water

736   Conservation 27(02), 123-127+135. (in Chinese).

737   Luan, J. W., Liu, S. R., Chang, S. X., Wang, J. X., Zhu, X. L., Liu, K., Wu, J. H., 2014. Different

738   effects of warming and cooling on the decomposition of soil organic matter in warm–temperate

739   oak forests: a reciprocal translocation experiment. Biogeochemistry 121(3), 551-564.

740   https://doi.org/10.1007/s10533-014-0022-y.

741   Lv, J. T., Miao, Y. X., Huang, Z. Q., Han, R. X., Zhang, S. Z., 2018. Facet-Mediated Adsorption and

742   Molecular Fractionation of Humic Substances on Hematite Surfaces. Environmental Science

743   & Technology 52(20), 11660-11669. https://doi.org/10.1021/acs.est.8b03940.

744   Ma, L. W., Liu, L., Lu, Y. S., Chen, L., Zhang, Z. C., Zhang, H. W., Wang, X. R., Shu, L., Yang, Q. P.,

745   Song, Q. N., Peng, Q. H., Yu, Z. P., Zhang, J., 2022. When microclimates meet soil microbes:

746   Temperature controls soil microbial diversity along an elevational gradient in subtropical

747   forests. Soil Biology and Biochemistry 166, 108566.

748   https://doi.org/10.1016/j.soilbio.2022.108566.

749   Ma, X. Q., Heal, K. V., Liu, A. Q., Jarvis, P. G., 2007.

750   Nutrient cycling and distribution in different-aged plantations of Chinese fir in   southern

751   China. Forest Ecology and Management 243(1), 61-74.

752   https://doi.org/10.1016/j.foreco.2007.02.018.

753 Marschner, B., Kalbitz, K., 2003. Controls of bioavailability and biodegradability of dissolved

754 organic matter in soils. Geoderma 113(3-4), 211-235.

755 https://doi.org/10.1016/S0016-7061(02)00362-2.

756 Melendez-Perez, J. J., Martínez-Mejia, M. J., Eberlin, M. N., 2016. A reformulated aromaticity

757 index equation under consideration for non-aromatic and non-condensed aromatic cyclic

758 carbonyl compounds. Organic Geochemistry 95, 29-33.

759 https://doi.org/10.1016/j.orggeochem.2016.02.002.

760 Mladenov, N., Zheng, Y., Miller, M. P., Nemergut, D. R., Legg, T., Simone, B., Hageman, C.,

761 Rahman, M. M., Ahmed, K. M., McKnight, D. M., 2010. Dissolved organic matter sources and

762 consequences for iron and arsenic mobilization in Bangladesh aquifers. Environmental

763 Science & Technology 44(1), 123-128. https://doi.org/10.1021/es901472g.

764 Mo, Y. Y., Peng, F., Gao, X. F., Xiao, P., Logares, R., Jeppesen, E., Ren, K. X., Xue, Y. Y., Yang, J.,

765 2021. Low shifts in salinity determined assembly processes and network stability of

766 microeukaryotic plankton communities in a subtropical urban reservoir. Microbiome 9, 128.

767 https://doi.org/10.1186/s40168-021-01079-w.

768 Navarrete, A. A., Soares, T., Rossetto, R., van Veen, J. A., Tsai, S. M., Kuramae, E. E., 2015.

769 Verrucomicrobial community structure and abundance as indicators for changes in chemical

770 factors linked to soil fertility. Antonie van Leeuwenhoek 108(3), 741-752.

771 https://doi.org/10.1007/s10482-015-0530-3.

772 Nunan, N., Schmidt, H., Raynaud, X., 2020. The ecology of heterogeneity: soil bacterial

773 communities and C dynamics. Philosophical Transactions of The Royal Society B 375,

774 20190249. http://doi.org/10.1098/rstb.2019.0249.

775 Osterholz, H., Singer, G., Wemheuer, B., Daniel, R., Simon, M., Niggemann, J., Thorsten, D., 2016.

776 Deciphering associations between dissolved organic molecules and bacterial communities in a

777 pelagic marine system. ISME Journal 10, 1717–1730. https://doi.org/10.1038/ismej.2015.231.

778 Qi, Y. L., Xie, Q. R., Wang, J. J., He, D., Bao, H. Y., Fu, Q. L., Su, S. H., Sheng, M., Li, S. L., Volmer,

779 D. A., Wu, F. C., Jiang, G. B., Liu, C. Q., Fu, P. Q., 2022. Deciphering dissolved organic matter

780 by Fourier transform ion cyclotron resonance mass spectrometry (FT-ICR MS): from bulk to

781 fractions and individuals. Carbon Research, 1, 3. https://doi.org/10.1007/s44246-022-00002-8.

782 Qiu, L., Fang, W. W., He, H. Z., Liang, Z. W., Zhan, Y. Y., Lu, Q. H., Liang, D. W., He, Z. L., Mai, B.

783   X., Wang, S. Q., 2020. Organohalide-Respiring Bacteria in Polluted Urban Rivers Employ

784   Novel Bifunctional Reductive Dehalogenases to Dechlorinate Polychlorinated Biphenyls and

785   Tetrachloroethene. Environmental Science & Technology 54(14), 8791-8800.

786   https://doi.org/10.1021/acs.est.0c01569.

787 R Core Team, 2018. R: A language and environment for statistical computing.

788 Ren, C. J., Zhou, Z. H., Guo, Y. X., Yang, G. H., Zhao, F. Z., Wei, G. H., Han, X. H., Feng, L., Feng,

789   Y. Z., Ren, G. X., 2020. Contrasting patterns of microbial community and enzyme activity

790   between rhizosphere and bulk soil along an elevation gradient. Catena 196, 104921.

791   https://doi.org/10.1016/j.catena.2020.104921.

792 Roth, V.-N., Lange, M., Simon, C., Hertkorn, N., Bucher, S., Goodall, T., Griffiths, R. I.,

793   Mellado-Vázquez, P. G., Mommer, L., Oram, N. J., Weigelt, A., Dittmar, T., Gleixner, G., 2019.

794   Persistence of dissolved organic matter explained by molecular changes during its passage

795   through soil. Nature Geoscience 12(9), 755-761.   https://doi.org/10.1038/s41561-019-0417-4.

796 Rustad, L. E., 2008. The response of terrestrial ecosystems to global climate change: Towards an

797   integrated approach. Science of The Total Environment 404(2-3), 222-235.

798   https://doi.org/10.1016/j.scitotenv.2008.04.050.

799 Sansupa, C., Wahdan, S. F. M., Hossen, S., Disayathanoowat, T., Wubet, T., Purahong, W., 2021.

800   Can We Use Functional Annotation of Prokaryotic Taxa (FAPROTAX) to Assign the

801   Ecological Functions of Soil Bacteria? Applied Sciences 11(2), 688.

802   https://doi.org/10.3390/app11020688.

803 Schmidt, M. W. I., Torn, M. S., Abiven, S., Dittmar, T., Guggenberger, G., Janssens, I. A., Kleber,

804   M., Kogel-Knabner, I., Lehmann, J., Manning, D. A. C., Nannipieri, P., Rasse, D. P., Weiner, S.,

805   Trumbore, S.E., 2011. Persistence of soil organic matter as an ecosystem property. Nature 478,

806   49-56. https://doi.org/10.1038/nature10386.

807 Shen, J., Liang, Z. Y., Kuzyakov, Y., Li, W. T., He, Y. T., Wang, C. Q., Xiao, Y., Chen, K., Sun, G.,

808   Lei, Y. B., 2023. Dissolved organic matter defines microbial communities during initial soil

809   formation after deglaciation. Science of The Total Environment, 878, 163171.

810   https://doi.org/10.1016/j.scitotenv.2023.163171.

811 Swenson, T. L., Bowen, B. P., Nico, P. S., Northen, T. R., 2015. Competitive sorption of microbial

812 metabolites on an iron oxide mineral. Soil Biology and Biochemistry 90, 34-41.

813 https://doi.org/10.1016/j.soilbio.2015.07.022.

814 Taketani, R. G., Lanconi, M. D., Kavamura, V. N., Durrer, A., Andreote, F. D., Melo, I. S., 2017.

815 Dry Season Constrains Bacterial Phylogenetic Diversity in a Semi-Arid Rhizosphere System.

816 Microbial Ecology 73 (1), 153-161. https://doi.org/10.1007/s00248-016-0835-4.

817 Tang, M. Z., Li, L., Wang, X. L., You, J., Li, J. N., Chen, X., 2020. Elevational is the main factor

818 controlling the soil microbial community structure in alpine tundra of the Changbai Mountain.

819 Scientific Reports 10, 12442. https://doi.org/10.1038/s41598-020-69441-w.

820 Trivedi, P., Anderson, I. C., Singh, B. K., 2013. Microbial modulators of soil carbon storage:

821 integrating genomic and metabolic knowledge for global prediction. Trends in Microbiology

822 21(12), 641-651. https://doi.org/10.1016/j.tim.2013.09.005.

823 Thevenot, M., Dignac, M. F., Rumpel, C., 2010. Fate of lignins in soils: A review. Soil Biology and

824 Biochemistry, 42(8), 1200-1211. https://doi.org/10.1016/j.soilbio.2010.03.017.

825 Triebwasser, D. J., Tharayil, N., Preston, C. M., Gerard, P. D., 2012. The susceptibility of soil

826 enzymes to inhibition by leaf litter tannins is dependent on the tannin chemistry, enzyme class

827 and vegetation history. New Phytologist, 196(4), 1122-1132.

828 https://doi.org/10.1111/j.1469-8137.2012.04346.x.

829 Wan, W. J., He, D. L., Li, X., Xing, Y. H., Liu, S., Ye, L. P., Njoroge, D. M., Yang, Y. Y., 2021.

830 Adaptation of *pho*D-harboring bacteria to broader environmental gradients at high elevations

831 than at low elevations in the Shennongjia primeval forest. Geoderma 401, 115210.

832 https://doi.org/10.1016/j.geoderma.2021.115210.

833 Wang, W. X., Tao, J. C., Yu, K., He, C., Wang, J. J., Li, P. H., Chen, H. M., Xu, B., Shi, Q., Zhang, C.

834 L., 2021. Vertical stratification of dissolved organic matter linked to distinct microbial

835 communities in subtropic estuarine sediments. Frontiers in Microbiology 12, 697860.

836 https://doi.org/10.3389/fmicb.2021.697860.

837 Wang, Y. H., Zhang, G. L., Wang, H. L., Cheng, Y., Liu, H., Jiang, Z., Li, P., Wang, Y. X., 2021.

838 Effects of different dissolved organic matter on microbial communities and arsenic

839 mobilization in aquifers. Journal of Hazardous Materials 411, 125146.

840   https://doi.org/10.1016/j.jhazmat.2021.125146.

841   Wang, S. J., Ruan, H. H., Wang, B., 2009. Effects of soil microarthropods on plant litter

842   decomposition across an elevation gradient in the Wuyi Mountains. Soil Biology and

843   Biochemistry 41(5), 891-897. https://doi.org/10.1016/j.soilbio.2008.12.016.

844   Witzgall, K., Vidal, A., Schubert, D. I., Höschen, C., Schweizer, S. A., Buegger, F., Pouteau, V.,

845   Chenu, C., Mueller, C. W., 2021. Particulate organic matter as a functional soil component for

846   persistent soil organic carbon. Nature Communications 12, 4115.

847   https://doi.org/10.1038/s41467-021-24192-8.

848   Wu, D., Zhang, M. M., Peng, M., Sui, X., Li, W., Sun, G. Y., 2019. Variations in Soil Functional

849   Fungal Community Structure Associated With Pure and Mixed Plantations in Typical

850   Temperate Forests of China. Frontiers in Microbiology 10, 1636.

851   https://doi.org/10.3389/fmicb.2019.01636.

852   Wu, M., Li, P. F., Li, G. L., Petropoulos, E., Feng, Y. Z., Li, Z. P., 2021. The chemodiversity of

853   paddy soil dissolved organic matter is shaped and homogenized by bacterial communities that

854   are orchestrated by geographic distance and fertilizations. Soil Biology and Biochemistry 161,

855   108374. https://doi.org/10.1016/j.soilbio.2021.108374.

856   Wu, W. X., Lu, H. P., Sastri, A., Yeh, Y. C., Gong, G. C., Chou, W. C., Hsieh, C. H., 2018.

857   Contrasting the relative importance of species sorting and dispersal limitation in shaping

858   marine bacterial versus protist communities. ISME Journal, 12(12) 485-494.

859   https://doi.org/10.1038/ismej.2017.183.

860   Wu, X. J., Liu, P. F., Wegner, C. E., Luo, Y., Xiao, K. Q., Cui, Z. L., Zhang, F. S., Liesack, W., Peng,

861   J. J., 2021. Deciphering microbial mechanisms underlying soil organic carbon storage in a

862   wheat-maize rotation system. Science of The Total Environment 788, 147798.

863   https://doi.org/10.1016/j.scitotenv.2021.147798.

864   Wu, X. Q., Wu, L. Y., Liu, Y. N., Zhang, P., Li, Q. H., Zhou, J. Z., Hess, N. J., Hazen, T. C., Yang, W.

865   L, Chakraborty, R., 2018. Microbial interactions with dissolved organic matter drive carbon

866   dynamics and community succession. Frontiers in Microbiology 9, 1234.

867   https://doi.org/10.3389/fmicb.2018.01234.

868   Wu, Z. Y., Lin, W. X., Li, J. J., Liu, J. F., Li, B. L., Wu, L. K., Fang, C. X., Zhang, Z. X., 2016.

869   Effects of seasonal variations on soil microbial community composition of two typical zonal

870   vegetation types in the Wuyi Mountains. Journal of Mountain Science 13(6), 1056-1065.

871   https://doi.org/10.1007/s11629-015-3599-2.

872   Xun, W. B., Li, W., Xiong, W., Ren, Y., Liu, Y. P., Miao, Y. Z., Xu, Z. H., Zhang, N., Shen, Q. R.,

873   Zhang, R. F., 2019. Diversity-triggered deterministic bacterial assembly constrains community

874   functions. Nature Communications 10, 3833. https://doi.org/10.1038/s41467-019-11787-5.

875   Ye, Q. H., Wang, Y. H., Zhang, Z. T., Huang, W. L., Li, L. P., Li, J. T., Liu, J. S., Zheng, Y., Mo, J.

876   M., Zhang, W., Wang, J. J., 2020. Dissolved organic matter characteristics in soils of tropical

877   legume and non-legume tree plantations. Soil Biology and Biochemistry 148, 107880.

878   https://doi.org/10.1016/j.soilbio.2020.107880.

879   Yuan, M. M., Guo, X., Wu, L. W., Zhang, Y., Xiao, N. J., Ning, D. L., Shi, Z., Zhou, X. S., Wu, L.

880   Y., Yang, Y. F., Tiedje, J. M., Zhou, J. Z., 2021.

881   Climate warming enhances microbial network complexity and stability. Nature Climate

882   Change, 11(4), 343-U100. https://doi.org/10.1038/s41558-021-00989-9.

883   Yun, Y., Gui, Z. Y., Su, T. Q., Tian, X. F., Wang, S. J., Chen, Y., Su, Z. Y., Fan, H. Q., Xie, J. X., Li,

884   G. Q., Xia, W. J., Ma, T., 2022. Deep mining decreases the microbial taxonomic and functional

885   diversity of subsurface oil reservoirs. Science of The Total Environment 821, 153564.

886   https://doi.org/10.1016/j.scitotenv.2022.153564.

887   Zeng, X. M., Feng, J., Chen, J., Delgado-Baquerizo, M., Zhang, Q. G., Zhou, X. Q., Yuan, Y. S.,

888   Feng, S. H., Zhang, K. X., Liu, Y. R., Huang, Q. Y., 2022. Microbial assemblies associated

889   with temperature sensitivity of soil respiration along an altitudinal gradient. Science of The

890   Total Environment, 820, 153257. https://doi.org/10.1016/j.scitotenv.2022.153257.

891   Zhang, J., Zhang, B. G., Liu, Y., Guo, Y. Q., Shi, P., Wei, G. H., 2018.

892   Distinct large-scale biogeographic patterns of fungal communities in bulk soil and soybean rh

893   izosphere in China. Science of The Total Environment 644, 791-800.

894   https://doi.org/10.1016/j.scitotenv.2018.07.016.

895   Zhang, Y. L., Heal, K. V., Shi, M. J., Chen, W. X., Zhou, C. F., 2022. Decreasing molecular diversity

896   of soil dissolved organic matter related to microbial community along an alpine elevation

897   gradient. Science of The Total Environment 818, 151823.

898   https://doi.org/10.1016/j.scitotenv.2021.151823.

899 Zhou, J. Z., Ning, D. L., 2017. Stochastic Community Assembly: Does It Matter in Microbial

900   Ecology? Microbiology and Molecular Biology Reviews 81(4), e00002-17.

901   https://doi.org/10.1128/MMBR.00002-17.

902 Zhou, L., Bai, C. R., Cai, J., Hu, Y., Shao, K. Q., Gao, G., Jeppesen, E., Tang, X. M., 2018. Bio-cord

903   plays a similar role as submerged macrophytes in harboring bacterial assemblages in an

904   eco-ditch. Environmental Science and Pollution Research 25(26), 26550-26561.

905   https://do.iorg/10.1007/s11356-018-2697-4.

906 Zhou, X. R., Chen, X. K., Qi, X. N., Zeng, Y. Y., Guo, X. W., Zhuang, G. Q., Ma, A. Z., 2023. Soil

907   bacterial communities associated with multi-nutrient cycling under long-term warming in the

908   alpine meadow. Frontiers in Microbiology, 14, 1136187.

909   https://doi.org/10.3389/fmicb.2023.1136187.

910 Zhu, D., Ma, J., Li, G., Rillig M. C., Zhu, Y. G., 2021. Soil plastispheres as hotpots of antibiotic

911   resistance genes and potential pathogens. The ISME Journal 16(2), 521-532.

912   https://doi.org/10.1038/s41396-021-01103-9.

913 Zhuang, T. C., Lin, P., Chen, R.H., 1997. Seasonal Variation on Amounts and Groups of

914   Heterotrophic Microorganisms in Forest Soil at Wuyishan National Nature Reserve. Journal of

915   Xiamen University (Natural Science) 35(4), 655-658. (in Chinese).

916

917

918 **Author Contributions**

919 All authors contributed to the study conception and design**. Shuzhen Wang**: Investigation,

920 Validation, Data Curation, Data analysis, Writing - first draft; **Kate V. Heal**: Supervision, Writing -

921 review & editing; **Qin Zhang**: Validation, Data analysis; **Yuanchun Yu**: Supervision; **Mulualem**

922 **Tigabu**: Reading and polishing the manuscript; **Shide Huang**: Soil sampling, **Chuifan Zhou**:

923 Conceptualization, Visualization, Resources, Supervision. All authors commented on previous

924 versions of the manuscript. All authors read and approved the final manuscript.

925

926 **Acknowledgments**

930

931   **Figure captions**

932   **Fig. 1.** Inter sample rankings analysis of common-shared DOM molecules in five vegetation zones

933   along the elevation gradient in the Wuyi Mountains, Fujian Province, China. Codes for the

934   different vegetation zones - EB: evergreen broad-leaved forest; CB: coniferous and broad-leaved

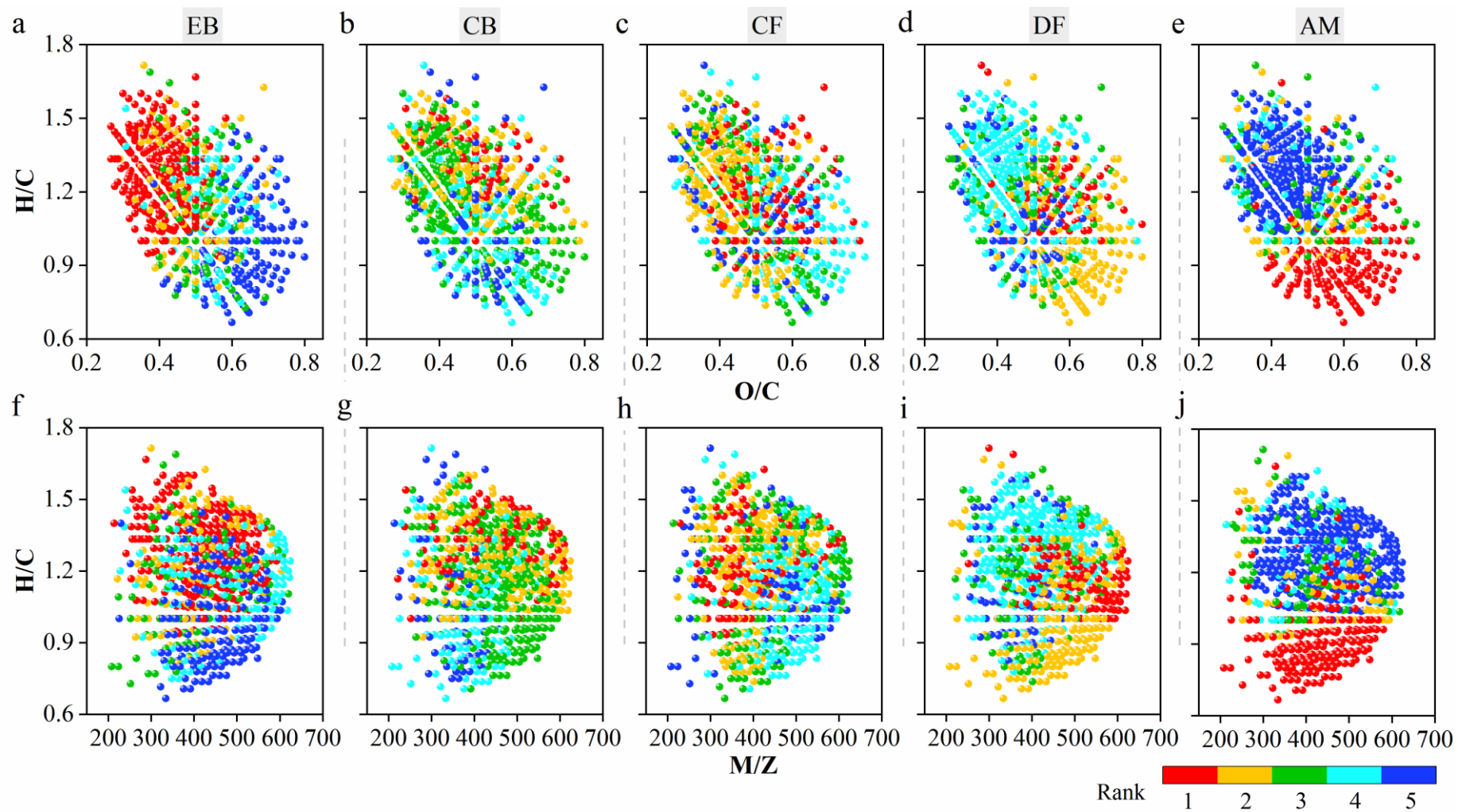935   mixed forest; CF: coniferous forest; DF: subalpine dwarf forest; AM: alpine meadow.

936

937   **Fig. 2.** Co-occurring network diagrams for soil bacteria (a) and fungi (b) (top 300 OTUs) across

938   all soil samples along the elevation gradient in the Wuyi Mountains, Fujian Province, China. The

939   box below each of (a) and (b) contains summary characteristics of the results of 10,000 random

940   networks generated for bacteria and fungi, respectively, according to the Erdös–Réyni model. Fit

941   of Sloan's neutral community model (NCM) to the OTUs of the soil (c) bacterial and (d) fungal

942   community assemblies for all soil samples. The solid black line represents the best-fitting neutral

943   model and the dashed black lines represent the 95% confidence intervals around it. Blue points

944   between the dashed black lines represent OTUs that follow the neutral process. The green and

945   orange points indicate OTUs that occur more and less frequently than predicted by the NCM,

946   respectively. R^2 indicates the fit to the NCM, m is the estimated migration rate, and Nm is the

947   product of metacommunity size and m values. (e) Bar plots of the modified stochasticity ratio

948   (MST) values of the soil bacterial and fungal community assemblies in different vegetation zones

949   along the elevation gradient. The horizontal dashed purple line (MST = 0.5) was set as the

950   boundary between deterministic (MST < 0.5) and stochastic (MST > 0.5) assembly processes.

951   Values are means ± standard error (n = 3). Different lowercase letters for bacteria/fungi indicate

952   significant differences between vegetation zones at different elevations according to LSD tests (P

953   < 0.05). See Fig. 1 for explanation of the codes for the different vegetation zones.
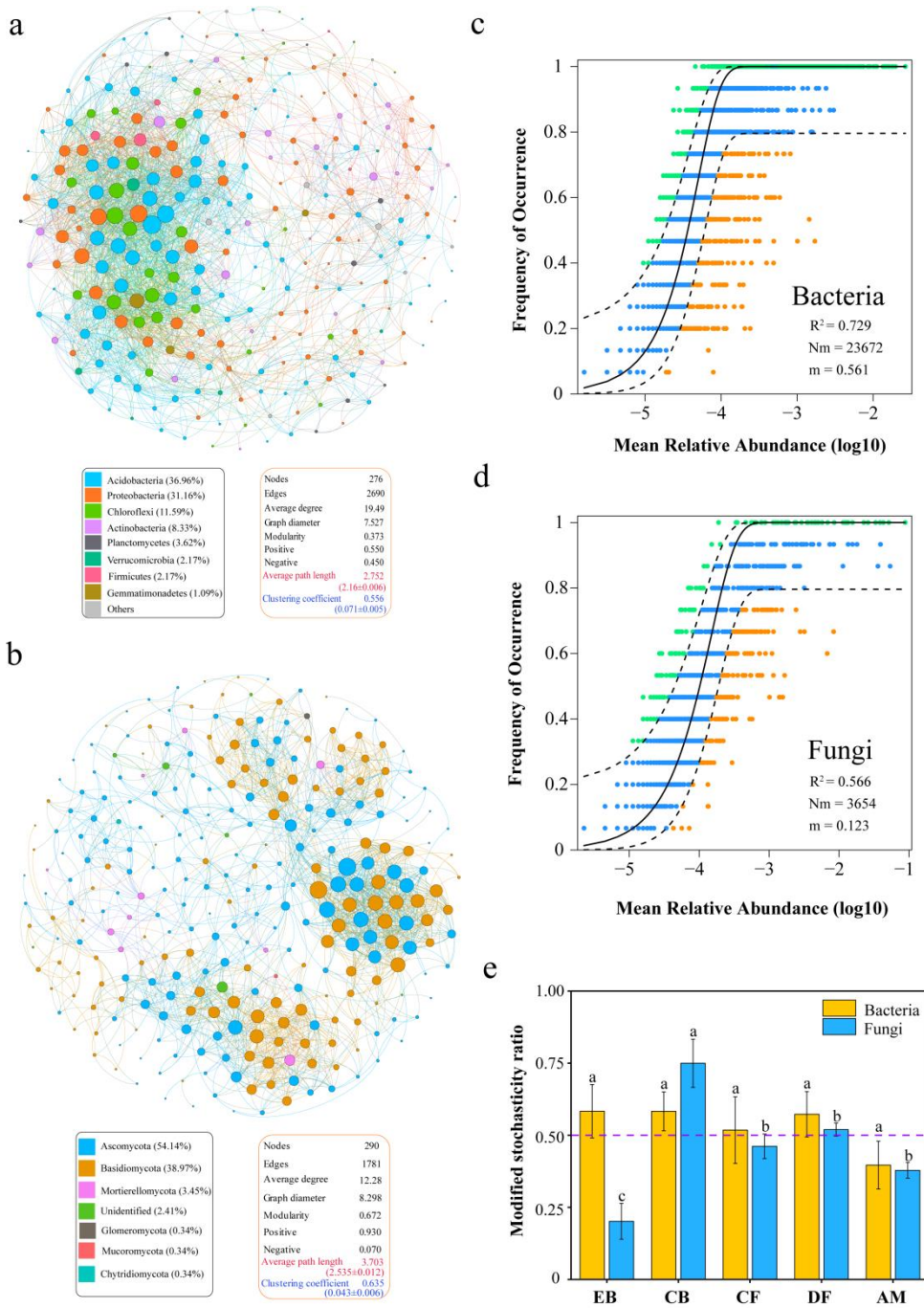
954

Fig. 3. (a) Heatmap of correlation between microbial community characteristics (Chao1, Shannon and Faith's PD indices, modified stochasticity ratio (MST)) and site elevation and DOM components/characteristics (defined in Supplementary Material Section S1). *, $0.01 \leq P < 0.05$; **, $0.001 \leq P < 0.01$ indicate significant coefficients. Co-occurrence network diagrams of significant ($P < 0.01$) correlations between the 100 most abundant soil DOM molecular formulae and the 100 highest relative abundance OTUs for bacteria (b) and fungi (c) in soil samples across the elevation gradient of different vegetation zones. Blue circles represent the OTUs of bacterial and fungal phyla. Green and red circles represent the lignin/CRAM-like structure and tannin molecules, respectively. The sizes of the circles indicate the relative abundance of the OTUs and DOM molecular formulae. The blue and red lines indicate significant positive and negative correlations, respectively, between DOM formulae and microbial phyla.
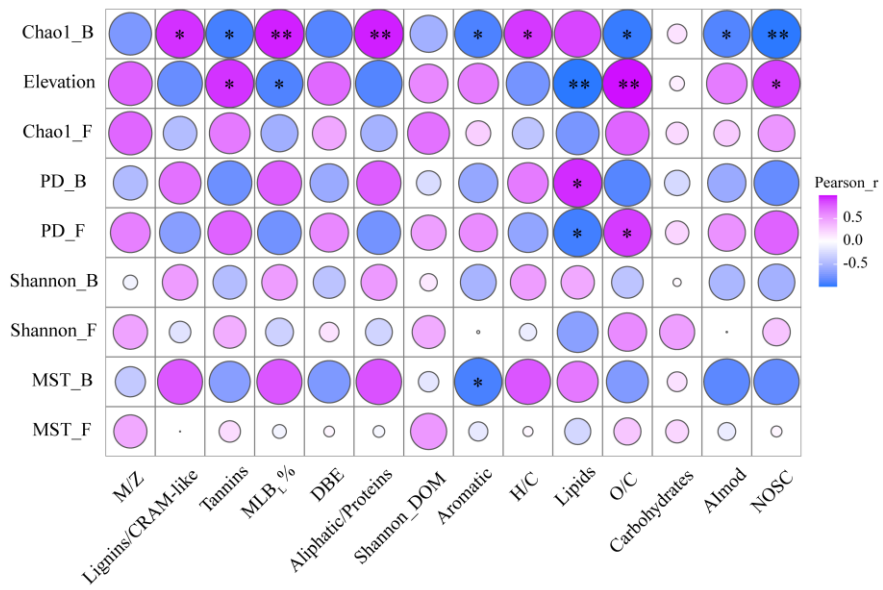
Fig. 4. Random forest (RF) analysis to identify the importance of different microbial predictors of the multiple nutrient cycling (MNC) index of the 15 soil samples along an elevation gradient in the Wuyi Mountains, Fujian Province, China. (a) Bacterial community predictors: relative abundance of the 10 most abundant bacterial phyla, alpha diversity indices (Shannon index, Chao1 index, Faith's PD index), the site pH, and elevation. (b) Fungal community predictors: relative abundance of the 3 most abundant fungal phyla, alpha diversity indices (Shannon index, Chao1 index, Faith's PD index), the site pH, and elevation. Partial least squares path models (PLS-PM) showing the effects of soil microbial communities characteristics on MNC (c). The line width is proportional to the magnitude of the path coefficient. Numbers adjacent to arrows indicate the direct effect size of the relationship. The black and blue lines indicate positive and negative path coefficient, respectively. R^2 indicates the variance of the dependent variable explained by the model. GOF is the goodness-of-fit index of the model. *, $0.01 \leq P < 0.05$; **, $0.001 \leq P < 0.01$; ***, $P < 0.001$ indicate significant predictors or path coefficients.
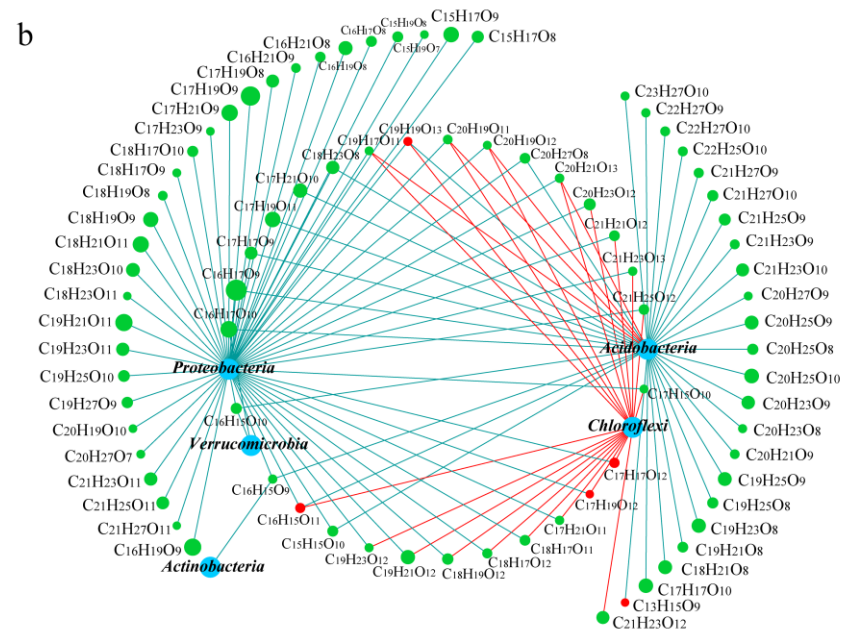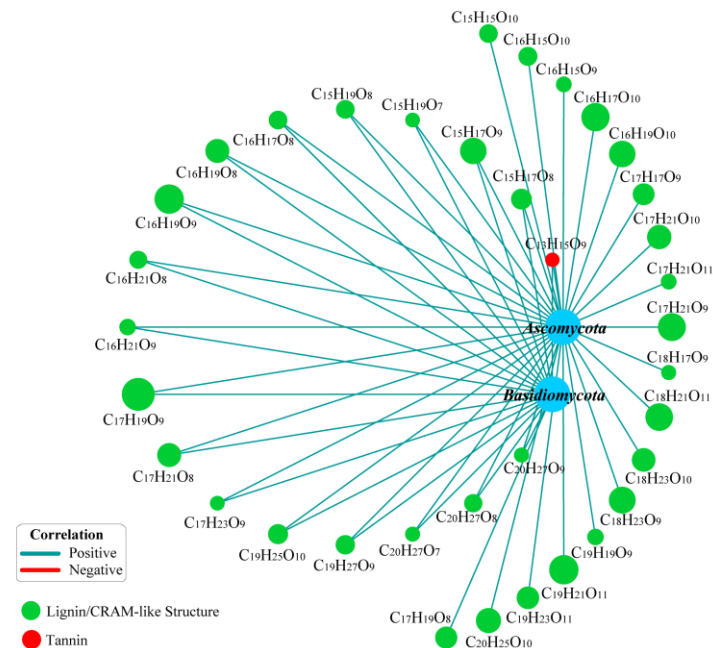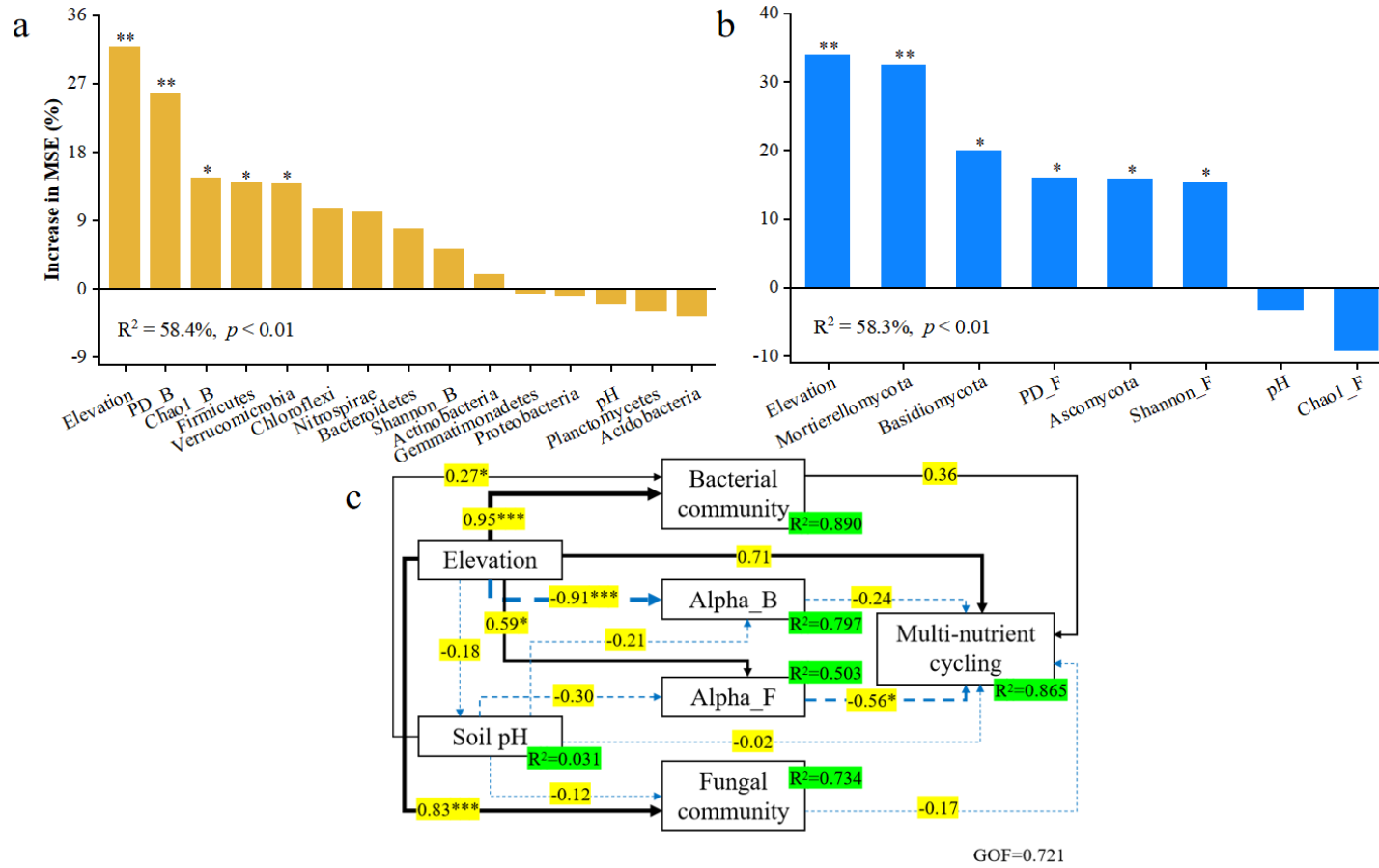
Fig. 2

a

■ Acidobacteria (36.96%)	
■ Proteobacteria (31.16%)	
■ Chloroflexi (11.59%)	
■ Actinobacteria (8.33%)	
■ Planctomycetes (3.62%)	
■ Verrucomicrobia (2.17%)	
■ Firmicutes (2.17%)	
■ Gemmatimonadetes (1.09%)	
■ Others	

Nodes	276
Edges	2690
Average degree	19.49
Graph diameter	7.527
Modularity	0.373
Positive	0.550
Negative	0.450
Average path length	2.752 (2.16±0.006)
Clustering coefficient	0.556 (0.071±0.005)

b

■ Ascomycota (54.14%)	
■ Basidiomycota (38.97%)	
■ Mortierellomycota (3.45%)	
■ Unidentified (2.41%)	
■ Glomeromycota (0.34%)	
■ Mucoromycota (0.34%)	
■ Chytridiomycota (0.34%)	

Nodes	290
Edges	1781
Average degree	12.28
Graph diameter	8.298
Modularity	0.672
Positive	0.930
Negative	0.070
Average path length	3.703 (2.535±0.012)
Clustering coefficient	0.635 (0.043±0.006)

c

Bacteria

$R^2 = 0.729$

Nm = 23672

m = 0.561

d

Fungi

$R^2 = 0.566$

Nm = 3654

m = 0.123

e

985
986 **Fig. 4**

987

990 **Table 1.** Soil properties in different vegetation zones along an elevation gradient in the Wuyi Mountains, Fujian Province, China. All data are presented as means $\pm$

991 standard error ($n = 3$). EB: evergreen broad-leaved forest; CB: coniferous and broad-leaved mixed forest; CF: coniferous forest; DF: subalpine dwarf forest; AM:

992 Alpine meadow). Ammoniacal-nitrogen (NH_4^+-N); nitrate-nitrogen (NO_3^--N); available phosphorus (AP); available potassium (AK); dissolved organic carbon (DOC);

993 total nitrogen (TN); total carbon (TC); C/N ratio: TC/TN; MNC: soil multiple nutrient cycling index, calculated as explained in Section 2.5. NO_3^--N, NH_4^+-N, and

994 DOC reported as mg kg^{-1} fresh weight. Different lowercase letters in a row indicate significant differences between elevations ($P < 0.05$).

Soil property	Vegetation zone and elevation				
	EB (290 m)	CB (1070 m)	CF (1400 m)	DF (1800 m)	AM (1960 m)
pH	4.70±0.04ab	4.64±0.09ab	4.58±0.04ab	4.55±0.04b	4.73±0.03a
NH_4^+-N (mg kg^{-1})	12.71±0.64a	15.23±1.70a	13.38±0.28a	14.23±0.62a	18.20±2.18a
NO_3^--N (mg kg^{-1})	1.89±0.60a	1.11±0.04a	1.99±0.10a	1.48±0.21a	1.37±0.11a
AP (mg kg^{-1})	5.38±1.09b	5.11±0.49b	11.64±4.89ab	7.95±0.41ab	11.67±0.93a
AK (mg kg^{-1})	156.96±15.91ab	113.33±16.53b	130.85±20.32b	200.07±7.48a	223.74±16.17a
DOC (mg kg^{-1})	54.28±4.06c	56.21±8.07c	93.93±9.80ab	80.08±4.71b	109.43±4.36a
TN (g kg^{-1})	1.47±0.26c	1.20±0.55c	3.42±0.21b	4.53±0.30b	6.96±0.67a
TC (g kg^{-1})	20.88±1.23cd	19.29±7.70d	45.53±1.54bc	60.29±3.12ab	98.15±14.76a
C/N	14.78±1.78a	16.80±0.89a	13.36±0.39a	13.36±0.50a	14.01±1.34a
MNC	0.22±0.03c	0.16±0.07c	0.41±0.03b	0.43±0.02b	0.68±0.08a

Table 2. Intensity weighted average (wa) values of the different characteristics of DOM molecules and relative abundance of different element combinations from

soils along an elevation gradient, Wuyi Mountains, Fujian Province, China. $n = 1$ as a composite sample for the three plots at each elevation was analyzed by FT-ICR

MS. DBE: double bond equivalent; NOSC: average nominal oxidation state of carbon; AI_{mod}: modified aromaticity index; MLB_L: molecular lability boundary. The

calculation methods are described in Supplementary Material Section S4. Vegetation zone codes are as given in Table 1.

Vegetation zone code and elevation	DBE wa	M/Z wa	H/C wa	O/C wa	NOSC wa	AI_{mod} wa	MLB_L %	Shannon index	Characteristics of soil DOM molecules		
									CHO %	CHON %	CHOS %
EB (290 m)	8.49	409.15	1.25	0.48	-0.26	0.25	14.47	6.78	88.39	8.12	3.48
CB (1070 m)	9.20	439.60	1.21	0.52	-0.16	0.26	11.63	7.42	90.43	5.54	4.03
CF (1400 m)	8.37	414.03	1.24	0.53	-0.13	0.24	11.44	6.70	80.17	9.46	10.37
DF (1800 m)	10.20	455.60	1.13	0.55	0.004	0.29	7.96	7.60	86.79	7.83	5.39
AM (1960 m)	11.59	453.73	0.98	0.57	0.19	0.39	3.20	7.45	88.53	10.91	0.56

999
1000
1001

1002